Hindawi
Advances in Materials Science and Engineering
Volume 2020, Article ID 7814324, 18 pages
https://doi.org/10.1155/2020/7814324

Research Article

A Comparative Study of Antibacterial Activity of CuO/Ag and ZnO/Ag Nanocomposites

R. B. Asamoah,[1] E. Annan,[1] B. Mensah,[1] P. Nbelayim,[1] V. Apalangya,[2] B. Onwona-Agyeman,[1] and A. Yaya[1]

[1]*Department of Materials Science & Engineering, School of Engineering Sciences, CBAS, University of Ghana, Legon, Accra, Ghana*
[2]*Department of Food Process Engineering, School of Engineering Sciences, CBAS, University of Ghana, Legon, Ghana*

Correspondence should be addressed to A. Yaya; ayaya@ug.edu.gh

Received 16 April 2020; Revised 12 May 2020; Accepted 18 May 2020; Published 19 June 2020

Academic Editor: Victor M. Castaño

The synergistic effects of transition metal based nanocomposites are known to possess enhanced antibacterial activities. However, in-depth analysis of the relative antibacterial performance of some of the prominent nanocomposites remains unavailable. This study compares the antibacterial activity of two separate nanocomposites, which are copper oxide with silver (CuO/Ag) and zinc oxide with silver (ZnO/Ag). The individual CuO/Ag and ZnO/Ag nanocomposites were synthesised by a mixed wet-chemical method. The resulting particles were analysed by XRD, XRF, TEM, UV-Vis spectrophotometer, BET, and FTIR. The antibacterial activity of the nanoparticles were tested on Gram-negative and Gram-positive bacteria, *Escherichia coli* (ATCC25922) and *Staphylococcus aureus* (ATCC25923), respectively, using the Kirby–Bauer disc diffusion and the microdilution methods. The Kirby–Bauer disc diffusion test results had the same minimum inhibition concentration (MIC) value for both CuO/Ag and ZnO/Ag against *E. coli* and *S. aureus*, which was 0.25 mg/ml. The applied nanocomposites using microdilution showed that CuO/Ag had approximately 98.8% and 98.7% efficiency on the respective Gram-positive and Gram-negative bacterial species, while ZnO/Ag achieved 91.7% and 89.3% efficiency, respectively, against the Gram-positive and Gram-negative bacterial species. This study presents a novel approach for relative analysis of the performance efficiency of transition metal based nanocomposites.

1. Introduction

Inorganic nanoparticles have demonstrated strong activity against broad-spectrum Gram-positive and Gram-negative bacterial species [1]. The toxicity of nanoparticles to bacteria depends on the kind and composition of the nanoparticles as well as the type of bacteria involved [2]. Silver has shown superior antibacterial activity among the family of inorganic nanoparticles [3]. Silver nanoparticles are effective against a wide span of microbes including Gram-positive and Gram-negative bacteria and viruses [4]. The antibacterial activity of silver is dependent on the antibacterial mechanistic routes of nanoparticles against bacterial species [5]. These routes are (1) the mediating of reactive oxygen species (ROS), which may destabilize cell functionality or integrity, and (2) the direct penetration of nanoparticles, which may cause functional and structural changes to organelles [6]. Several researchers have proposed the strong interaction of ionic silver with thiol groups of important microbial enzymes, which disrupts their structure and causes them to be inactive as one of the main reasons for silver's high antibacterial activity [7]. It has also been proposed that once bacteria are treated with silver, their DNA replication function is lost. Moreover, there is experimental evidence showing profound structural changes in the cell membrane of bacteria once treated with silver [8].

However, in comparison with other inorganic nanoparticles, silver is very expensive [9]. Moreover, a major drawback of using silver nanoparticles is due to their associated small size, which enables them to cross biological membranes with ease of posing risks to humans and the environment. Inorganic nanoparticles such as zinc oxide

(ZnO) and copper oxide (CuO) are cheaper, widely available, less toxic to mammalian cells, stable, and more environmentally friendly [10–12]. Therefore, in order to ensure a fair balance between a potent antibacterial inorganic material and cost effectiveness of the material, a nanocomposite consisting of silver and other tested inorganic antibacterial material is proposed [13]. Nanometal oxides including zinc oxide and copper oxide have demonstrated antibacterial activity [14]. It is envisaged that nanocomposites of silver with each of these metal oxides will create a potent and yet more cost-effective inorganic antibacterial material [15]. The nanocomposites to be created would therefore be a separate silver with copper oxide (CuO/Ag) and silver with zinc oxide (ZnO/Ag) nanocomposites. The synergistic combination of these nanocomposites would enhance their antibacterial potential. In this case, each elemental composition of the nanocomposite will harness its own antibacterial activity through the production of its associated ions, acting as antibacterial agents [16]. This study, therefore, presents nanocomposites of copper oxide with silver (CuO/Ag) and zinc oxide with silver (ZnO/Ag). The investigation undertakes the task of comparing their bioactivities by representative Gram-positive and Gram-negative bacterial species, which are, respectively, the *E. coli* strain ATCC25922 and *S. aureus* strain ATCC25923 obtained from the Noguchi Memorial Institute for Medical Research, University of Ghana, Legon.

2. Experimental

2.1. Materials. All reagents were of analytical grade and were used without further purification. Copper acetate (Cu(acetate), purity ≥99%), zinc acetate ((Zn(acetate), purity 99%), sodium hydroxide (NaOH, purity ≥99%), sodium borohydride ($NaBH_4$ purity ≥99%), and silver nitrate ($AgNO_3$, purity ≥99%) were all purchased from Sigma-Aldrich.

2.2. Synthesis of Nanocomposites

2.2.1. Synthesis of Copper Oxide/Silver Nanocomposite. Copper oxide/silver (CuO/Ag) nanocomposites were synthesised by the wet chemical precipitation synthesis method. By this approach, 0.1 M copper acetate was dissolved in a 100 ml of deionised water. The solution was continuously stirred at 700 rpm on a magnetic stirrer hot plate at 80°C. A homogeneous solution was shortly formed. 2 M NaOH was added dropwise to reach a pH of 11. The synthesis was continuously stirred at the same speed and temperature for a further sixty minutes. A black suspension was formed, which is indicative of the formation of copper oxide. To form the CuO/Ag nanocomposite, 0.001 M of silver nitrate was added to the 100 ml of CuO aqueous precipitate at the same temperature and stirring speed. 5 ml of 0.004 M of sodium borohydride was added dropwise to the reacting solution for the reduction of silver ions. The temperature was gradually reduced to room temperature at the same stirring speed. The synthesised nanocomposites were separated by centrifugation and washed several times with distilled water to remove excess ions. The particles obtained were dried in an oven at 80°C overnight. Then they were calcined at 500°C to remove impurities that may be present on particles surfaces. The particles were subsequently characterised and applied for antibacterial activities.

$$\left(\mathbf{Cu^{2+}} + \mathbf{NaOH}\right)\mathbf{aq} \rightleftharpoons \mathbf{CuO} + \mathbf{H_20} \quad (1)$$

$$\left(\mathbf{Ag^{+}} + \mathbf{e^{-}}\right)\mathbf{aq} \rightleftharpoons \mathbf{Ag^{0}} \quad (2)$$

$$\left(\mathbf{CuO} + \mathbf{Ag^{0}}\right)\mathbf{aq} \rightleftharpoons \frac{\mathbf{CuO}}{\mathbf{Ag^{0}}} \quad (3)$$

where equations (1) and (2) describe the formation of copper oxide and reduced silver nanoparticles, respectively. Nanocomposite of copper oxide and silver is formed in (3).

2.2.2. Synthesis of Zinc Oxide/Silver Nanocomposite. Similarly, surfactant-free zinc oxide/silver nanocomposites were synthesised by the wet chemical precipitation method. 0.1 M zinc acetate was dissolved in a 100 ml of deionised water. A homogeneous solution was obtained after keeping the solution at 700 rpm on a hot magnetic stirrer plate at 80°C. The temperature and stirring speed were kept throughout the synthesis period. 2 M NaOH was added to the homogeneous solution to increase its pH to 11. A white precipitate was formed, which was stirred at the same speed and temperature for another sixty minutes. The synthesis process continued by the rapid addition of 0.001 M silver nitrate to the aqueous zinc oxide precipitate. Subsequently, 5 ml of 0.004 M sodium borohydride was then added dropwise to form reduced silver nanoparticles in the composite. The synthesis was allowed to continue for another sixty minutes, during which the temperature was allowed to gradually fall to ambient conditions. The fabricated nanocomposites were separated by centrifugation at 6000 rpm. The particles were severally washed to remove unreacted ions. They were dried at 80°C overnight and further calcined at 500°C for 3 hours at a heating rate of 1°C/S. The synthesised particles were successively analysed through a series of characterizations and utilized for antibacterial studies.

$$\left(\mathbf{Zn^{2+}} + \mathbf{NaOH}\right)\mathbf{aq} \rightleftharpoons \mathbf{ZnO} + \mathbf{H_20} \quad (4)$$

$$\left(\mathbf{Ag^{+}} + \mathbf{e^{-}}\right)\mathbf{aq} \rightleftharpoons \mathbf{Ag^{0}} \quad (5)$$

$$\mathbf{ZnO} + \mathbf{Ag^{0}} \rightleftharpoons \frac{\mathbf{ZnO}}{\mathbf{Ag^{0}}} \quad (6)$$

Equations (4) to (6) are a sequence of steps for the formation of zinc oxide/silver (ZnO/Ag) nanocomposite.

2.3. Antibacterial Testing. The as-prepared nanocomposites (CuO/Ag and ZnO/Ag) were tested on *E. coli* and *S. aureus*. The Kirby–Bauer disk diffusion and the microdilution using optical density methods were employed for antibacterial testing. All materials used for the antibacterial testing were

sterilized at 121°C for 15 minutes. All the microbiology applications were done in a sterile laminar flow cabinet.

2.3.1. Disk Diffusion Assay. The bacteria were separately cultured overnight in a Mueller–Hinton broth. 100 ul of separate bacteria cultures containing approximately 6×10^7 CFU was uniformly streaked on a solidified Mueller–Hinton agar in a glass Petri dish. Paper disks measuring about 6 mm were individually impregnated with CuO/Ag or ZnO/Ag at varying concentrations of 5 mg/ml, 2 mg/ml, 1 mg/ml, 0.5 mg/ml, 0.25 mg/ml, 0.1 mg/ml, and 0 mg/ml. The concentration of 0 mg/ml was adopted as the control for the experiment. The impregnated paper disks were distinctly placed on the agar plates streaked with distinct bacteria. The agar plates were incubated overnight at 37°C. Visible zones of inhibition observed around the perimeter of the nanocomposite impregnated paper disks were measured and recorded for analysis of antibacterial activity.

2.3.2. Bacteria Growth Kinetic Assay. The disk diffusion antibiotic test presented a method for exploring the efficacy of CuO/Ag and ZnO/Ag on bacteria strains. However, the growth kinetics of bacteria are highly dependent on their optical density. Spectrophotometric technique was used to study the optical density of bacteria cell cultures to determine their growth kinetics. The Varioskan LUX multimode microplate reader (Thermo Fisher Scientific, USA) was employed for reading the optical densities of bacteria in a 96-well microplate. Separate bacteria cultures of *E .coli* and *S. aureus* were grown in a Mueller–Hinton broth to obtain an optical density of 0.2 corresponding to a bacteria density of 6×10^7 CFU. The bacteria inoculum was transferred into a 96-well microplate. CuO/Ag and ZnO/Ag were separately dispersed in an aqueous suspension by an ultrasonicator (Bransonic Ultrasonic Bath, Thomas Scientific, USA) operating at 60 s at 75 % amplitude at a pulse configuration of 0.5/0.5 s. The homogeneously dispersed nanocomposites were added to the respective bacteria inoculum. The bacteria were incubated for 24 hours at 37°C. The optical density of the inoculum was measured periodically during the culturing period to observe the bacteria growth state pattern by changes in the optical density. The data obtained from the spectrophotometric fluorescent reading were analysed to understand the kinetics of bacteria growth. Such information is fundamental to gaining in-depth knowledge on the antibacterial efficiency of silver nanocomposites.

3. Results and Discussion

3.1. Characterization of Nanocomposites

3.1.1. X-Ray Diffraction (XRD) Analysis of Metal Oxide/Silver Nanocomposite. All nanocomposites including copper oxide/silver (CuO/Ag) and zinc oxide/silver (ZnO/Ag) were studied with the X-ray diffractometer. The analysis was important to observe the prevalent crystal structure in the individual nanocomposites.

XRD was used to analyse the crystal structures of the synthesised copper oxide/silver (CuO/Ag) nanocomposites. The sharpness of the spectra is an indication of the crystalline nature of the nanocomposites. The XRD spectrum of synthesised CuO/Ag nanocomposite is presented in Figure 1. The main planes of CuO are (110), (002), (−111), (111), (200), (−112), (−200), (112), (020), (202), (−113), (022), (−311), (113), (220), (311), (004), (−222), and (−204). The corresponding 2θ diffraction of the planes occurred at 32.66, 35.49, 35.69, 38.86, 39.11, 46.40, 48.92, 51.50, 53.73, 58.47, 61.70, 66.06, 66.57, 68.07, 68.44, 72.73, 75.13, 75.59, and 80.48. The spectra peaks of copper oxide correlated with the spectra peaks of the CuO/Ag nanocomposite. The crystal structure analysis showed that the monoclinic phase of copper oxide was the dominant phase in the nanocomposite. The spectra peak of silver is weak due to the low concentration of silver in the nanocomposite. Silver has a face centered cubic (FCC) crystal structure. The unit cell has perpendicular faces with equal lengths along all sides. Silver atoms are located at each corner of the unit cell and at the middle of each face. The absence of unwanted peaks indicates the purity of the nanocomposite. The purity of the samples that were further analysed by X-ray fluorescence (XRF) is critical to determine the true antibacterial effect of the nanocomposite antibacterial agents. Using the Scherer equation, the crystallite size of CuO/Ag was calculated to be 34.2 nm.

The ZnO/Ag nanocomposite spectra shown in Figure 2 recorded the following diffraction peaks at 2θ: 31.80, 34.45, 36.29, 47.58, 56.66, 62.91, 66.45, 68.02, 69.16, 72.62, and 77.05. The respective planes of the diffraction peaks are (100), (002), (101), (102), (110), (103), (200), (112), (201), (004), and (202). The spectra peaks corresponded with the exact patterns of zinc oxide, which again signifies the purity of the nanocomposite. The spectra peak at 2θ of 38° is the (111) plane of silver. Silver had weak peaks due to the low concentration of silver in the nanocomposite. Similar observation about the weak spectra peaks of silver due to low concentration in a nanocomposite has been previously observed [17]. The crystallite size of ZnO/Ag nanocomposite according to the Scherer equation was found to be 36.17 nm.

3.1.2. X-Ray Fluorescence (XRF) Analysis of Metal Oxide/Silver Nanocomposite. The elemental analysis of metal oxide/silver nanocomposites including separate CuO/Ag and ZnO/Ag showed the quantity of constituents contained in each individually analysed sample of CuO/Ag and ZnO/Ag. The constituent elements detected in the whole sample were expressed as oxides in relative percentage of all the elements present in the sample. The results for the XRF spectroscopy analysis of CuO/Ag are shown in Table 1. The XRF analysis of CuO/Ag shows that the sample had a high content of copper oxide (CuO) followed by silver (Ag). All elements were expressed in oxides; hence the silver was communicated as Ag_2O. The weak peaks of silver recorded by the XRD spectrum are confirmed by its low content verified by the XRF elemental analysis.

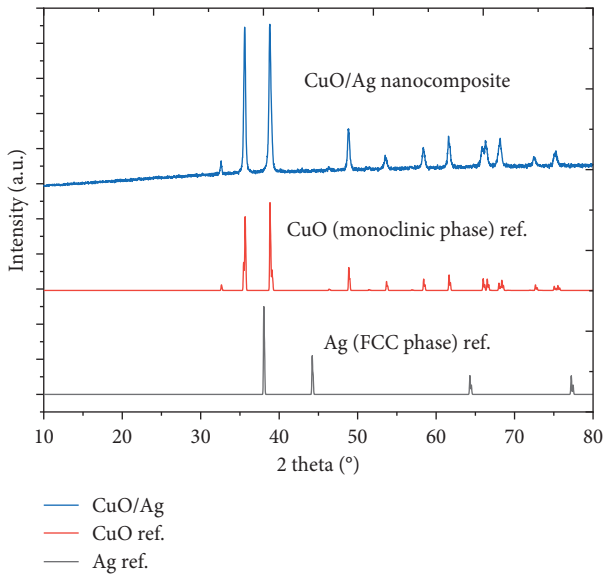

Figure 1: XRD spectrum of CuO/Ag correlated with the reference data of CuO monoclinic phase and the face centered cubic (FCC) phase of Ag.

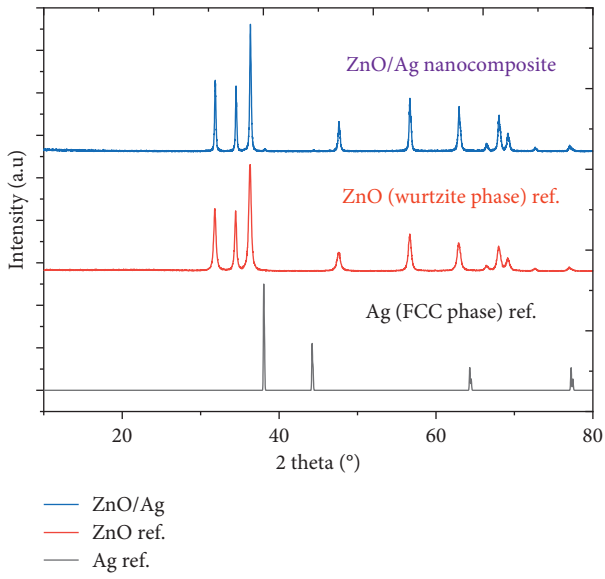

Figure 2: XRD pattern of ZnO/Ag nanocomposite in correlation with the wurtzite phase of ZnO and the face centered cubic (FCC) phase of Ag.

Table 1: XRF analysis of the components of copper oxide/silver and zinc oxide/silver (ZnO/Ag) nanocomposites.

Component	CuO/Ag	ZnO/Ag
Al2O3	0.0849	0.105
SiO2	0.147	0.257
P2O5	0.0146	0.0203
K2O	0.0429	0.0473
CaO	0.0214	0.0216
CuO	99.2	—
ZnO	—	98.8
Ag2O	0.518	0.547

The table also shows the XRF elemental analysis of ZnO/Ag. The highest constituent of the sample is zinc oxide followed by a low content of silver. The results agree with the weak peaks of silver in the XRD spectra pattern.

The XRF results revealed that the individual nanocomposites had similar respective compositions of metal oxides and silver.

3.1.3. Transmission Electron Microscope (TEM) Analysis of Metal Oxide/Silver Nanocomposites. The TEM micrographs of CuO/Ag and ZnO/Ag are, respectively, shown in Figures 3 and 4. CuO/Ag nanocomposite appears in nanorod shape. The respective length and width of the CuO/Ag nanorods were measured and plotted against their frequency. The silver component of the nanocomposite appears spherical, being supported by the copper oxides that are rather rod-shaped. A similar shape of nanorods has been observed among CuO nanoparticles [18]. As shown in Figure 3, CuO/Ag nanocomposites have an average length of 400 nm. The CuO/Ag nanocomposites have an average width of 20 nm. However, the size of the particles recorded by the X-ray diffraction was 34.2 nm. The dry CuO/Ag powder might have undergone agglomeration, which eventually influenced the sizes of its particles. CuO nanorods of similar size dimensions have demonstrated activity against a range of microbes [19].

The as-synthesized ZnO/Ag nanocomposites assumed a plate-like shape. This morphology is similar to that of other ZnO nanoparticles by Jang [20]. The size distribution of ZnO/Ag ranges from 15 nm to 60 nm with an average size of 35 nm. The size was similar to that computed by Scherer's equation, which was 36.17 nm. Such range of particle size is known to possess commended toxicity to bacteria species [21]. According to Scherer's equation performed on the highest intensity peak of the XRD spectra to compute the particle size, CuO/Ag and ZnO/Ag had similar sizes, which were 34.2 nm and 36.17 nm, respectively. The antibacterial activity of metal based nanoparticles among other factors is influenced by the size of the particle. Particle size influences the reactivity of the nanoparticle through the number of atoms available on the surface for reactivity. The number of atoms occupying the surface of a nanoparticle increases with decreasing size. The particle size affects other factors such as dissolution to produce associated ions mediating cell death. The cellular internalization of nanoparticles through cellular membranous pores leading to cell death is also highly dependent on particle size.

The similar range of sizes of the particles recorded by the XRD suggests that the separate particles had similar antibacterial effects with respect to their sizes.

3.1.4. UV-Vis Spectroscopy Analysis of Metal Oxide/Silver Nanocomposites. The UV-Vis (GENESYS 150 UV-Vis, Thermo Fisher Scientific, USA) spectrophotometric absorption spectra of CuO/Ag nanocomposites are found in Figure 5. CuO/Ag nanocomposite had highest wavelength peak at 542 nm. The excitation of electrons from the valence band to the conduction band of CuO/Ag is predominant at

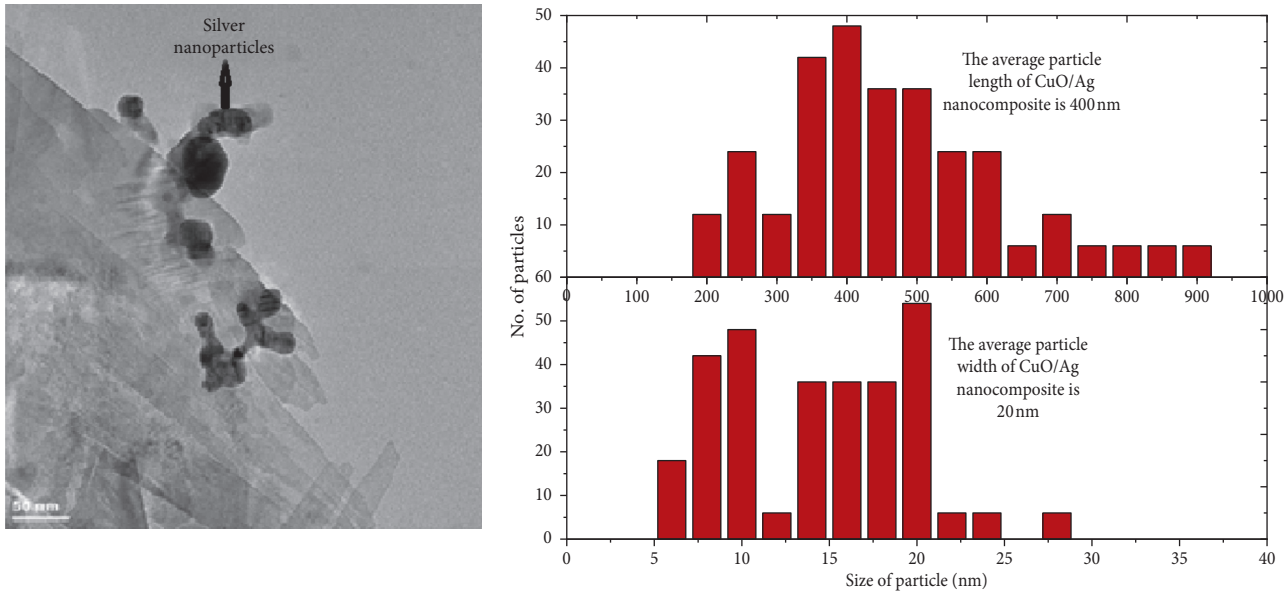

(a) (b)

Figure 3: (a) TEM micrograph of CuO/Ag. (b) Particle size distribution of CuO/Ag nanocomposite.

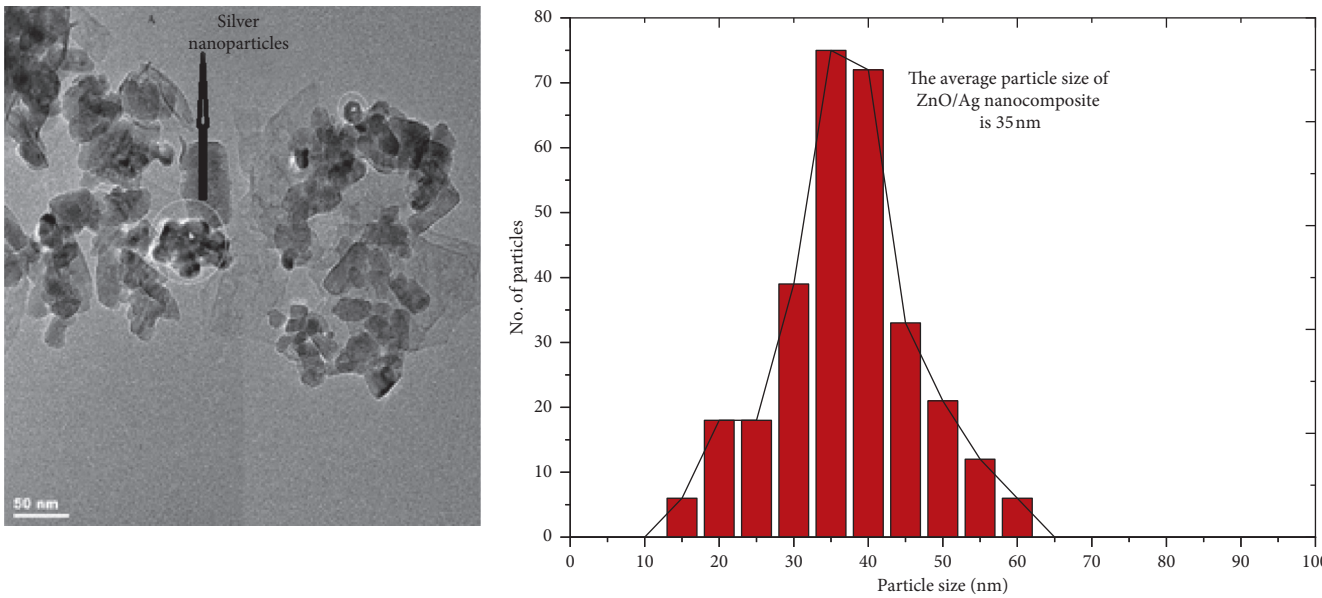

(a) (b)

Figure 4: (a) TEM micrograph of ZnO/Ag. (b) Particle size distribution of ZnO/Ag nanocomposite.

the peak wavelength [22]. The energy band gap of CuO/Ag nanocomposite is 1.2 eV. However, the energy band gap of CuO has previously been reported to be 1.54 eV [23]. The presence of silver enhances the band gap. Silver electrons act as dopants of CuO, which improves its energy band gap. Band gap enhancement affects the electrical conductivity of the resulting material. CuO/Ag with an energy band gap of 1.2 eV can cause the release of electrons at a lower energy wavelength than CuO, which had a band gap of 1.54 eV. The release of electrons by the nanoparticle is important for initiating cell death. The release electrons interact with bacteria cells or the fluid medium to produce reactive oxygen species (ROS), which become injurious to bacterial cells.

It is realised that UV-Vis of copper oxide/silver nanocomposite had a spectra peak extending from the UV range to the visible range. The copper oxide/silver particles could therefore extract energy from the UV or visible range of the spectrum. The acquisition of energy promotes electron transition preceding essential antibacterial activities of metal based nanomaterials such as copper oxide/silver

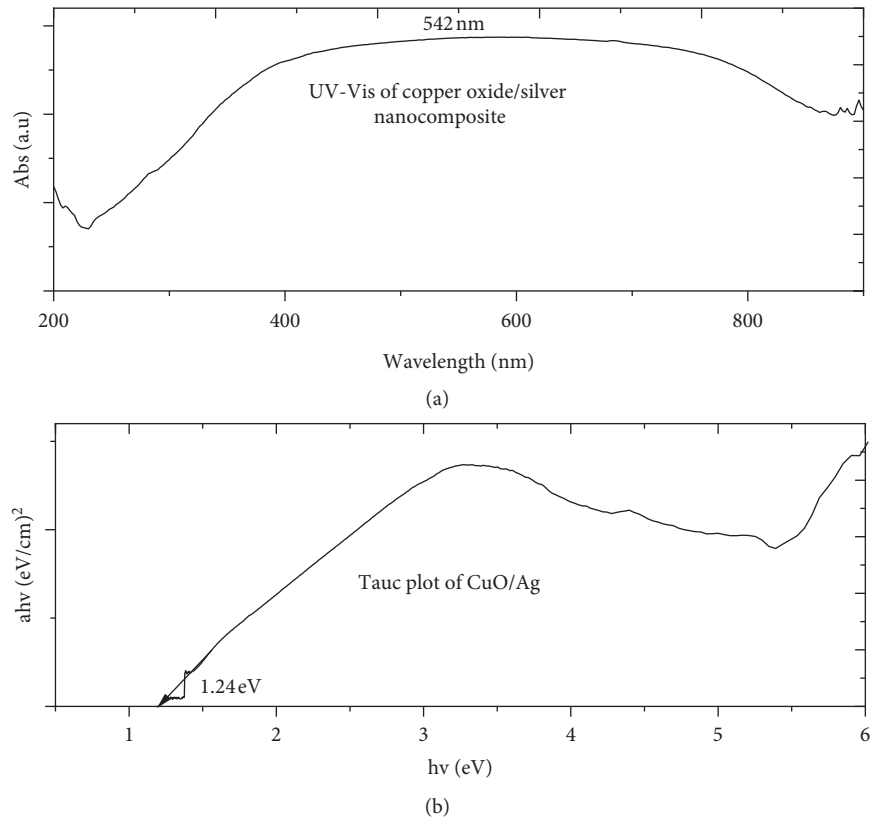

Figure 5: (a) UV-Vis spectrophotometric absorption spectra of CuO/Ag and (b) Tauc plot of CuO/Ag.

nanocomposites. In the presence of nanomaterials, the right incidence of the required energy causes the generation of reactive oxygen species.

ZnO/Ag nanocomposites are demonstrated in Figure 6. Absorption wavelength peak of 372 nm was recorded as the wavelength of energy for electron excitation in ZnO/Ag. Similar wavelength has been reported for ZnO [24]. This agrees with the predominance of the ZnO in the nanocomposite as revealed by the XRD and XRF results. The corresponding energy band gap was 2.88 eV. The energy band gap is lower than the traditionally reported band gap of zinc oxide, which is known to be 3-4 eV but mostly found to be 3.2 eV by a majority of researchers [23]. The enhanced band gap of ZnO/Ag is attributed to the presence of silver, which dopes the zinc oxide semiconductor, thereby enhancing its optical properties. The silver acted as a dopant to enhance the band gap of the ZnO particles. Band gap enhancement modifies the electrical conductivity of the ZnO particles. The band gap of ZnO/Ag recorded as 2.88 eV generates electrons at lower heat of light photon energy as compared to the band gap of the traditional band gap of ZnO, which is larger. Thus, it required lesser energy for electron transition, which accounts for cell death through the initiation of reactive oxygen species.

The phenomena might account for the high antibacterial activity of doped zinc oxide and that of other doped nanomaterials. Kumar and others demonstrated that doped zinc oxide exhibited higher antibacterial activity [25].

The lower energy band gap of CuO/Ag compared to ZnO/Ag means that the excitation of electrons in CuO/Ag would require a lower energy than ZnO/Ag. Also, according to the UV spectra, unlike CuO/Ag, ZnO/Ag did not have peak spectra within the visible range of the spectrum but rather within the UV range. Thus, ZnO/Ag would require higher energy for electron transition between energy states as compared to CuO/Ag, which recorded a broad spectra peak extending into the visible range of the spectrum. Electron transfer between energy states which principally occurs at the wavelength of the spectra peak creates electron excitation generating hole and electron pairs, resulting in reactive oxygen species that interact with bacteria species that are toxic to bacteria cells. CuO/Ag from the UV spectra analysis could be expected to cause cell death at a lower energy than ZnO/Ag, since it had spectra peak extending into the lower energy of the visible range.

3.1.5. Brunauer–Emmett–Teller (BET) Analysis of Clay-Nanocomposite Pellets. BET analysis was carried out to provide information on the surface area of the respective nanocomposites. The BET provided information on the surface area by the adsorption of nitrogen gas molecule as a function of relative adsorption pressure (P/P_0), which spans from 0.05 to 1. At ($P/P_0 = 1$), the gas molecules condense within the pores. As the pressure is decreased from its highest value of 1, gas desorption takes place. The process

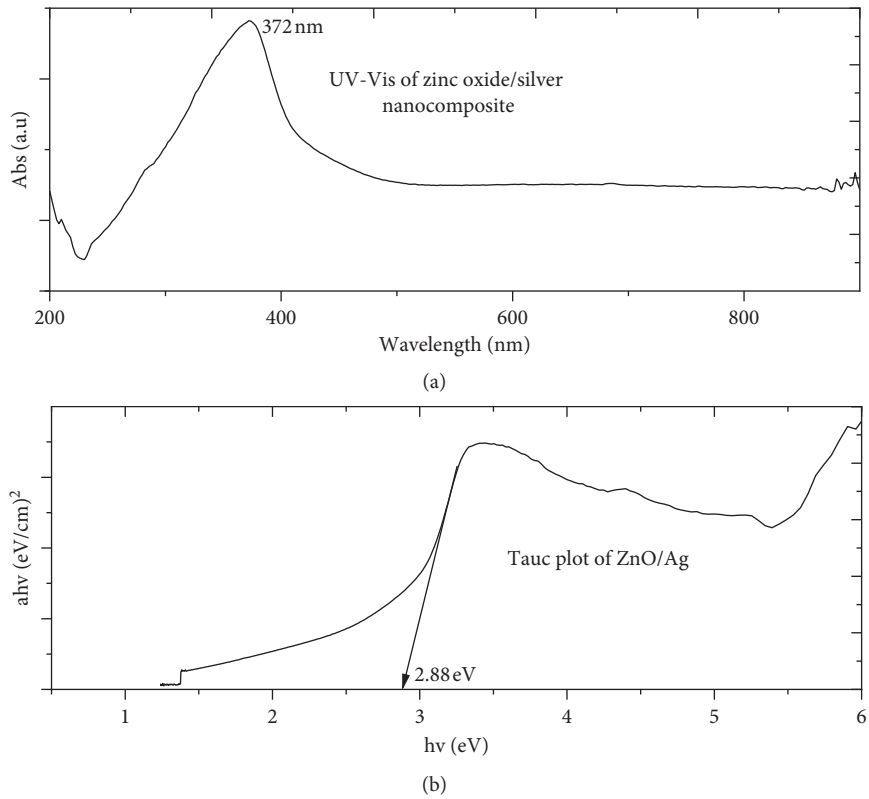

Figure 6: UV-Vis spectra of ZnO/Ag nanocomposite with its equivalent plot showing its energy band gap.

provides information on the adsorption-desorption of the gas molecules from the nanocomposite surfaces. The information is used to obtain properties about the material surface such as surface area, pore volume, and pore size distribution by the implementation of the BET equation. The adsorption-desorption curves are termed isotherms, which are classified into six different types depending on the IUPAC 1985 classification [26].

The analysis of surface area is crucial among the characteristics of nanomaterial based antibacterial agents. The larger the surface area of the nanomaterial, the greater its adsorption onto bacteria surfaces, thereby causing subsequent cell death. Surface area also increases with decreasing particle size. The smaller the particle size, the larger the surface area. Smaller particle sizes have demonstrated higher antibacterial activity [19]. The argument may be attributed to the fact that smaller particles by virtue of their size can easily penetrate into the cytoplasm through cellular pores. Particle size again influences reactivity. Decreasing the particle increases the reactivity because more atoms possessing free bonds become available on the surface for reactivity.

Figure 7 contains adsorption-desorption isotherm and the corresponding BJH (Barrett-Joyner-Halenda) plot describing its pore size distribution of CuO/Ag. The adsorption-desorption curve depicts a Type IV isotherm. Type IV isotherm is characteristic of pore sizes within the range of 1.5–100 nm. In Type IV isotherm, the micropores are filled at extremely low relative pressure. At the knee of the curve, a monolayer is formed, which is followed by a multilayer formation at a moderate pressure. As the pressure increases further, there is a condensation of gas molecules within pores. Gas adsorption continues at high relative pressure, which is an evidence of agglomeration confirming the aggregation already reported due to difference in particle size reported by XRD and TEM results.

The BJH plot confirms the Type IV isotherm of the CuO/Ag nanocomposite. The nanocomposite had pores ranging from micropores to mesopores, which is typical of Type IV isotherm. According to the BET equation, the surface area (S_{BET}) was calculated to be 18 m^2g^{-1}. Again, by applying the same BET equation, the pore volume of CuO/Ag was found to be 4.2 cm^3g^{-1}.

Figure 8 is the adsorption-desorption isotherms and the BJH plot of ZnO/Ag. The nitrogen adsorption and desorption at 77 K of ZnO/Ag nanocomposites behaved similarly to CuO/Ag. ZnO/Ag demonstrated a Type IV isotherm, in which the micropores were filled at extremely low relative pressure. At a low relative pressure at the knee of the isotherm curve monolayer of nitrogen gas was adsorbed on the ZnO/Ag surface. As the pressure increased to a moderate level, multilayer of adsorbed gas was formed, which condensed within pore structures at high pressures. At high pressure, gas adsorption continued.

The BJH plot of ZnO/Ag revealed that the nanocomposite possessed a range of pore sizes. The pores spanned from micropores to mesopores, which is characteristic of Type IV isotherms. The surface area (S_{BET}) of ZnO/Ag was found to be 18 m^2g^{-1}; the pore volume was found to be 4.0cm^3g^{-1}.

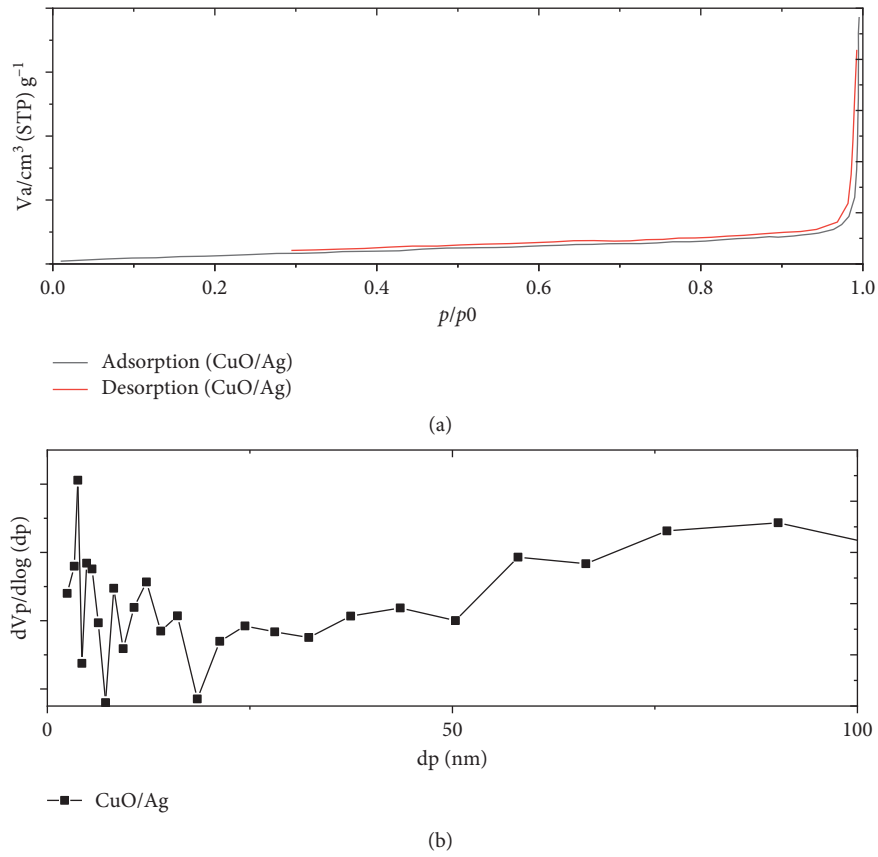

Figure 7: (a) Adsorption-desorption isotherms of nitrogen gas at 77 K and associated (b) BJH plot showing the pore size distribution of CuO/Ag.

Comparatively, ZnO/Ag and CuO/Ag possessed equivalent BET characteristic features. Their similarity in surface area suggests they had comparable particle size, which was also consistent with the XRD results of their particle size which suggested the same. Thus, ZnO/Ag and CuO/Ag have similar antibacterial activities with respect to their respective surface areas.

3.1.6. FTIR Analysis of Metal Oxide/Silver Nanocomposite. Fourier transform infrared (FTIR) spectroscopic analysis was carried out on the wet-chemical synthesised metal oxide/silver nanocomposites to ensure that surfactant free particles were used for the antibacterial studies. Surfactants are reported to influence the antibacterial activity. The FTIR analysis provided information on the surface properties on the respective nanocomposites. In this study, the FTIR spectra of CuO and ZnO are, respectively, consistent with those of CuO/Ag and ZnO/Ag, which is attributed to their high relative quantities as already demonstrated by the XRD and XRF analyses. Slight shifting in the wavenumber (cm^{-1}) of the bonds is attributed to the interactions between metal oxide (CuO or ZnO) and silver (Ag). Figure 9 shows the FTIR spectra analysis of CuO/Ag nanocomposite. Band at 572 cm^{-1} is attributed to Cu-O bond. The bands observed between 3600 and 3500 cm^{-1} indicate the presence of the O-H associated with water. Peaks corresponding to organic surfactants are absent because surfactant free nanocomposites were synthesised for testing on bacteria species to nullify any possible effects of surfactants in the antibacterial process.

Figure 10 illustrates the FTIR spectra of ZnO/Ag nanocomposite. The O-H bond that occurs with the spectra band of 3600 to 3500 cm^{-1} was very weak, which means that the moisture content was almost absent in this sample. The bond confirming the presence of zinc oxide was present at 694 cm^{-1}, which is the band for Zn-O bond. The weak bands occurring between 2920 and 1381 cm^{-1} are because of interaction with silver. Significant absorption peaks corresponding to organic molecules are not observed because the nanocomposites surfaces were void of surfactants. This was important to observe the true antibacterial activity of nanocomposites alone without any surfactant influences.

The surfactant free nanocomposites observed by FTIR analysis are in agreement with the high purity of the samples, which were also demonstrated by XRD and XRF analyses.

3.2. Antibacterial Study of CuO/Ag and ZnO/Ag against Bacteria Species

3.2.1. Disk Diffusion Studies. The antibacterial activities of CuO/Ag and ZnO/Ag nanocomposites were tested on *E. coli* and *S. aureus*, which are, respectively, Gram-negative and Gram-positive bacteria. Both CuO/Ag and ZnO/Ag nanocomposites showed activity on both bacteria species. The

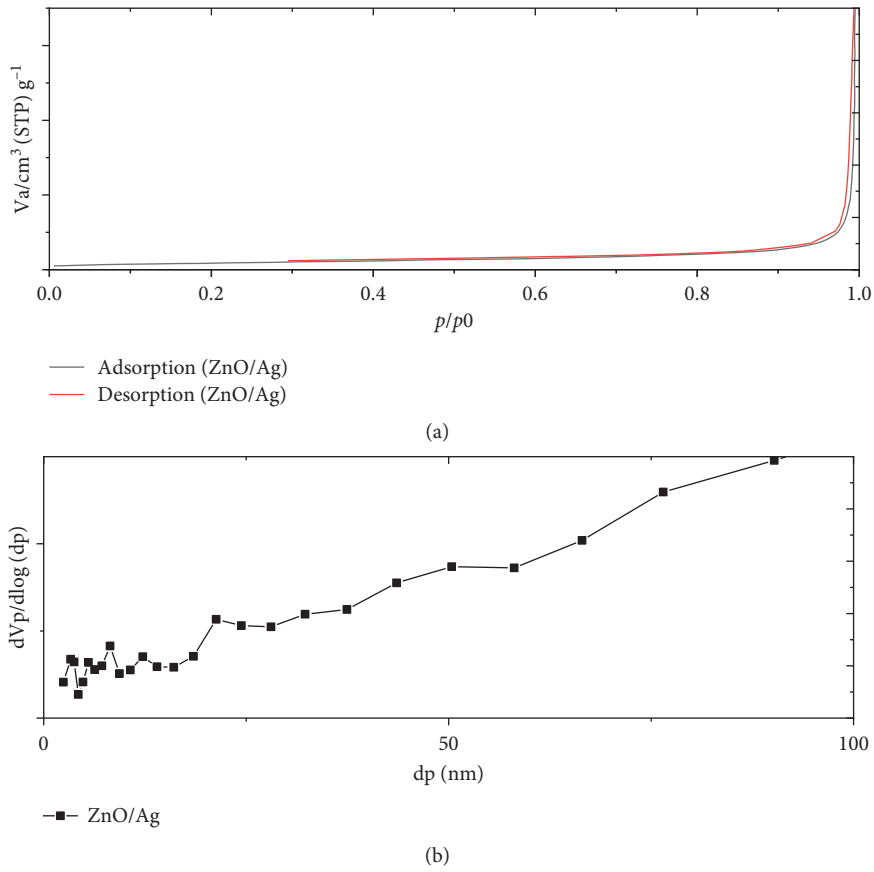

Figure 8: (a) Adsorption-desorption isotherms of nitrogen gas at 77 K and associated (b) BJH plot showing the pore size distribution of ZnO/Ag.

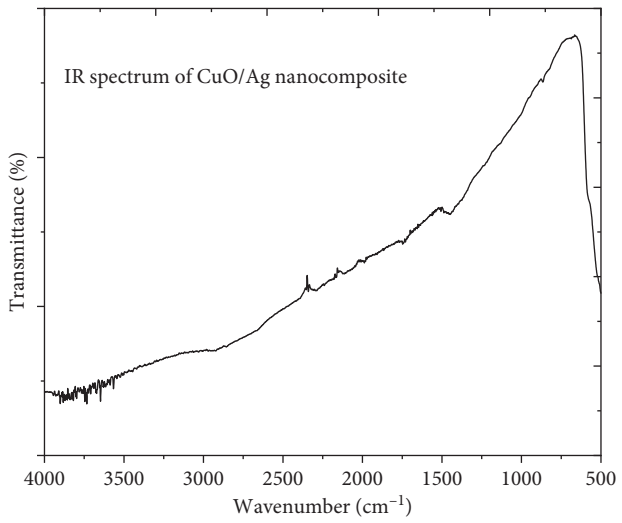

Figure 9: FTIR spectra analysis of CuO/Ag nanocomposite.

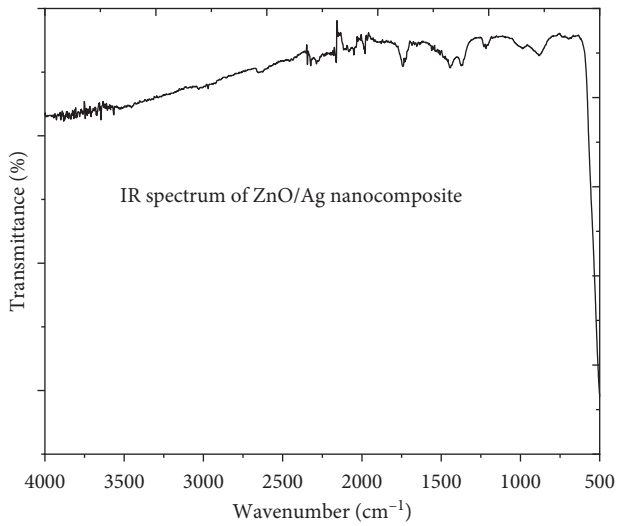

Figure 10: FTIR spectra analysis of ZnO/Ag nanocomposite.

enhanced antibacterial activity of the nanocomposites was attributed to silver. Silver, apart from other reasons, is reported as having comparatively high antibacterial activity [3]. The reason for the high antibacterial activity of silver has been reported by many researchers. They have suggested that the high affinity of silver for the sulphur in the thiol protein of bacteria is largely responsible for this [27]. The affinity leads to the breakage of disulphide bonds in thiols. The protein tertiary structure is eventually disrupted [28], resulting in cell death.

Figure 11 shows the antibiotic effect of CuO/Ag nanocomposite against *E. coli*. The zones of inhibition shows that CuO/Ag was effective against *E. coli* from a decreasing concentration of 5 mg/ml to 0.05 mg/ml. The MIC value of CuO/Ag against *E. coli* was 0.25 mg/ml. In previous work, the susceptibility of *E. coli* to Ag was high, while the same *E. coli* was resistive towards copper [29]. The literature report agrees with the finding in this study, in which the presence of silver in the nanocomposite demonstrates effectiveness against *E. coli*.

Similarly, in Figure 12, the activity of CuO/Ag against Gram-positive bacteria (*S. Aureus*) is demonstrated. The MIC was 0.25 mg/ml.

Figure 13 is a histogram of the summary of the activity of CuO/Ag on the Gram-negative and Gram-positive bacteria. The graph reveals that CuO/Ag nanocomposite was more effective against *S. aureus* than against *E. coli*. The observation can be made from the sizes of the inhibition zones of the respective strains of the bacteria species. The activity of CuO/Ag against *S. aureus* had relatively bigger zone of inhibition as compared to the activity of CuO/Ag against *E. coli*. The size of the inhibition zone depicts the sensitivity of the bacteria. A similar observation has already been reported by other researchers. It has been observed that Gram-positive bacteria such as *S. aureus* were more susceptible to antibiotics than the Gram-negative bacteria of *E. coli* [30]. Although *E. coli* had the smaller size of zone of inhibition, it had the same MIC as *S. aureus*, which was 0.25 mg/ml. This means that the same amount of CuO/Ag could result in a similar inhibition in both the *E. coli* and *S. aureus* strains. Strain specificity has been observed for *E. coli* among researchers [29]. While it was sensitive towards silver, it remained insensitive towards copper. Therefore, the effectiveness of the nanocomposite against *E. coli* was attributed to the presence of the composition of silver. The nanocomposite created a synergy which broadened its range of antibacterial spectrum. Therefore, it was effective against both Gram-negative and Gram-positive strains of the bacteria species.

ZnO/Ag nanocomposite was also tested on the two strains of bacteria species. First, ZnO/Ag was tested on *E. coli*. The results revealed that the ZnO/Ag nanocomposite was effective against *E. coli*. The activity of ZnO/Ag on *E. coli* can be observed in Figure 14. ZnO/Ag had an MIC value of 0.25 mg/ml.

Figure 15 shows the activity of ZnO/Ag against *S. aureus*. The zones of inhibition in this case are larger than those observed in ZnO/Ag against *E. coli* in Figure 14. This shows the higher efficiency of ZnO/Ag against *S. aureus* than against *E. coli*.

The antibacterial activity of ZnO/Ag on both *E. coli* and *S. aureus* is shown in Figure 16. Similar to the activities of CuO/Ag against *E. coli* and *S. aureus* strains, *S. aureus* was more susceptible than *E. coli*. The zones of inhibition of ZnO/Ag against *S. aureus* were comparatively bigger than those of ZnO/Ag against *E. coli*, which explains the higher activity of ZnO/Ag on *S. aureus* than on *E. coli*.

The antibacterial activities of CuO/Ag and ZnO/Ag against *E. coli* and *S. aureus* are compared in Figure 17. CuO/Ag concentrations of 5 mg/ml, 2 mg/ml, 1 mg/ml, 0.5 mg/ml, 0.25 mg/ml, 0.1 mg/ml, and 0 mg/ml against *E. coli* produced respective inhibition zones of 9 mm, 8 mm, 8 mm, 7 mm, 6 mm, 0 mm, and 0 mm. Its activity against *S. aureus* was 14 mm, 13 mm, 13 mm, 10 mm, 7 mm, 0 mm, and 0 mm. ZnO/Ag concentrations of 5 mg/ml, 2 mg/ml, 1 mg/ml, 0.5 mg/ml, 0.25 mg/ml, 0.1 mg/ml, and 0 mg/ml against *E. coli* produced respective inhibition zones of 8 mm, 7 mm, 7 mm, 7 mm, 7 mm, 0 mm, and 0 mm. Its activity against *S. aureus* was 12 mm, 12 mm, 10 mm, 9 mm, 8 mm, 0 mm, and 0 mm. The higher sensitivity of *S. aureus* was significant from its bigger zones of inhibition among the activities of each nanocomposite. Comparatively, the zones of CuO/Ag and ZnO/Ag had close values due to the influencing contribution of silver (Ag) in both nanocomposites. The Ag contribution is responsible for the common MIC of both nanocomposites for both species, which are indicated in Table 2. CuO/Ag had bigger zones in most instances, demonstrating its higher activity over ZnO/Ag.

3.2.2. Bacteria Growth Kinetic Study. The Kirby–Bauer disc diffusion bacteria susceptibility test was used to study the antibiotic efficiency of engineered silver/metal oxide (CuO/Ag and ZnO/Ag) nanocomposite. A major challenge with this technique is that it is difficult to determine the rate of antibacterial activity with respect to time [31]. In the disk diffusion technique, filter paper disk containing antibacterial agents is placed on an agar plate with bacteria spread on it. The antibacterial agents diffuse through the agar containing the bacteria [32]. The antibacterial potency is determined by the size of a zone of inhibition surrounding the filter paper disk after overnight incubation or approximately twelve hours of incubation. The size of the zone of inhibition produced in disk diffusion bacteria susceptibility technique is dependent on the amount of ions impregnated on the paper disc. The toxic ions interact with cells to cause cell death. The whole procedure takes approximately twelve hours to observe the resulting zone of inhibition. Thus, the disc diffusion method is not convenient for observing the time-kinetic effects of the antibacterial agents [33].

Antibacterial activity of nanoparticles involves a number of routes. Prominent among these routes are dissolution of nanoparticles to produce respective ions in solution, which are toxic to bacteria cells, nanoparticle interaction with bacteria cell walls, which disrupts the cell wall, and also the penetration of nanoparticles through cellular pores that bind to organelles, proteins, and genetic structures, which leads to cell death [6]. In the Kirby–Bauer disk diffusion method, it is difficult to differentiate between the ionic mediated cell death through the generation of reactive oxygen species and the nanoparticle-bacterial cell interaction. Diffusion typically involves the movement of ions rather than nanoparticles. In the disc diffusion approach, ionic mediated mechanistic pathway is popularly reported by a majority of researchers [34]. Other methods of antibacterial testing such as the broth microdilution present a modality of antibacterial testing which incorporates all possible routes of nanoparticle antibacterial mechanisms [35].

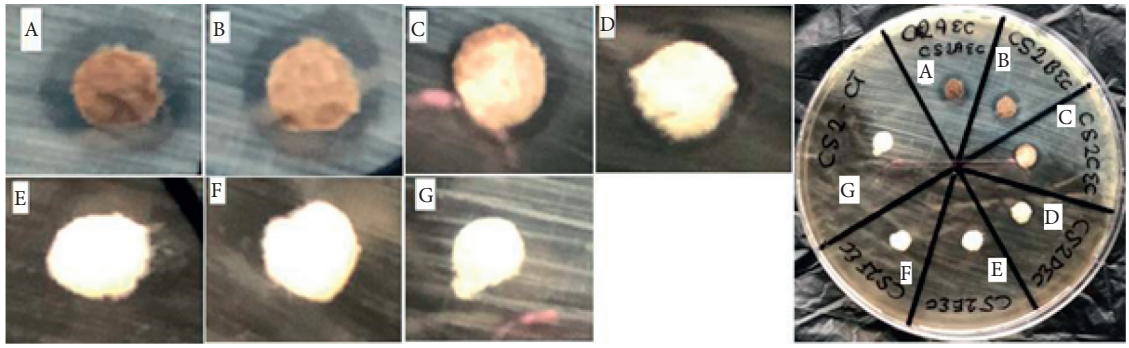

Figure 11: Antibacterial activity of CuO/Ag nanocomposite against *E. coli*. The paper disks were impregnated with the following suspension of copper oxide nanoparticles: A = 5 mg/ml, B = 2 mg/ml, C = 1 mg/ml, D = 0.5 mg/ml, E = 0.25 mg/ml, F = 0.1 mg/ml, and G = 0 mg/ml.

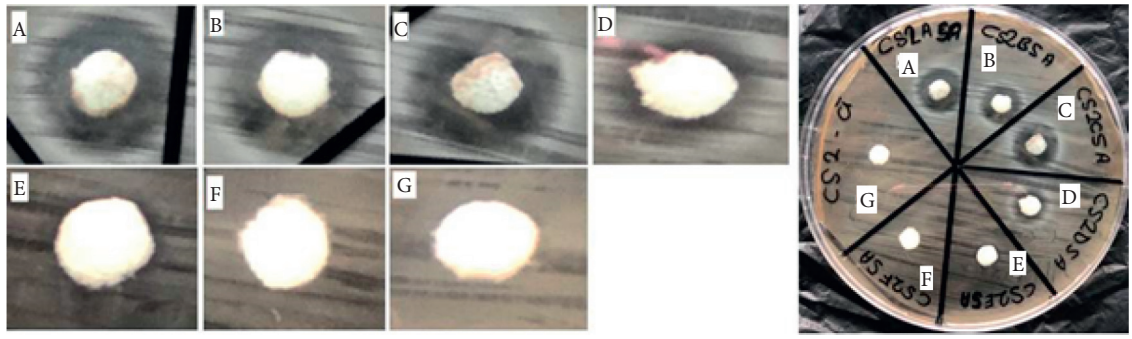

Figure 12: Antibacterial activity of CuO/Ag nanocomposite against *S. aureus*. The paper disks were impregnated with the following suspension of copper oxide nanoparticles: A = 5 mg/ml, B = 2 mg/ml, C = 1 mg/ml, D = 0.5 mg/ml, E = 0.25 mg/ml, F = 0.1 mg/ml, and G = 0 mg/ml.

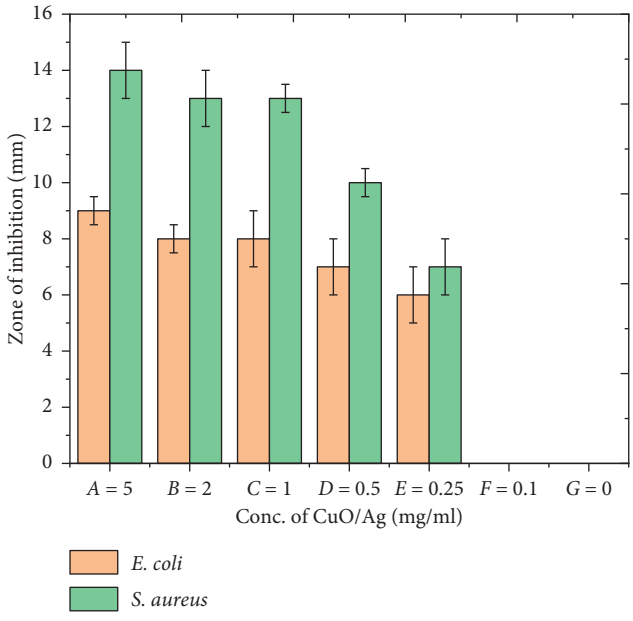

Figure 13: A histogram showing the activity of CuO/Ag nanocomposite against *E. coli* and *S. aureus*. A = 5 mg/ml, B = 2 mg/ml, C = 1 mg/ml, D = 0.5 mg/ml, E = 0.25 mg/ml, F = 0.1 mg/ml, and G = 0 mg/ml.

The broth microdilution technique is a liquid broth including a concentration of antibiotics and the bacteria to be tested [36]. In most cases, depending on the desired outcome, the antibiotics and the bacteria may be subject to varying concentrations. Broth microdilution allows the measurement of the optical density of the inoculum. The optical density value correlates with the quantity of bacteria present in the inoculum [21]. Hence, this technique, unlike disc diffusion, presents a quantitative method of measuring the bacteria growth with respect to time. The bacteria time-kinetics are important for analysing the time-dependency effect of antibacterial agents [37].

The bacteria growth kinetic studies of the antibacterial activity of CuO/Ag and ZnO/Ag nanocomposites were performed by distinctly subjecting *E. Coli* and *S. Aureus* bacteria cells to the inhibiting activities of the respective nanocomposites. The growth inhibition assay included a broth containing approximately $6 * 10^6$ CFU of respective bacteria cells with varying concentrations (1 mg/ml, 0.5 mg/ml, 0.25 mg/ml, 0.1 mg/ml, 0.05mg/ml, and 0 mg/ml) of the respective nanocomposite. A control experiment included that of a broth media with respective bacteria cells and no (0 mg/ml) antibacterial agent (zero amount of either of the individual nanocomposites). The optical density of the assay was initially and periodically measured. The optical density of broth media with the respective individual nanocomposite was used as a blank hence deducted from the optical density of the corresponding inoculum to obtain the actual optical density of only the respective bacteria cell. Therefore, the optical density obtained for analysis was the exact representative of bacteria growth time-kinetics.

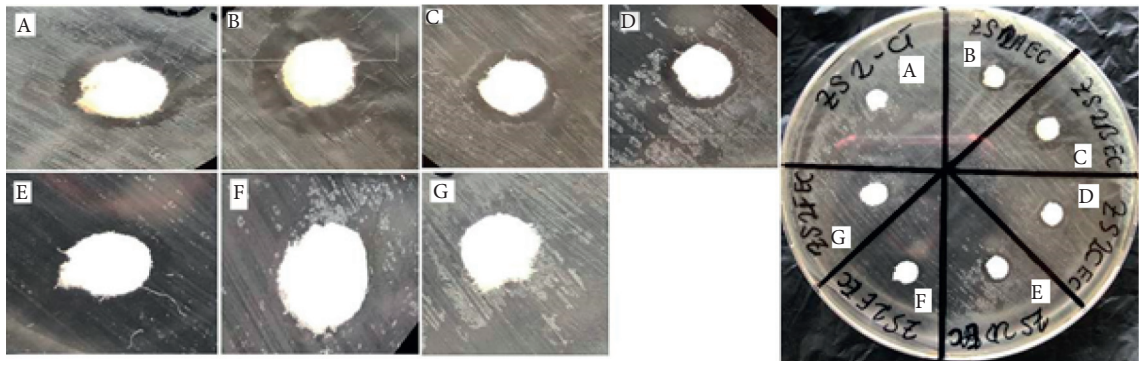

Figure 14: Antibacterial activity of ZnO/Ag nanocomposite against *E. coli*. The paper disks were impregnated with the following suspension of copper oxide nanoparticles: A = 5 mg/ml, B = 2 mg/ml, C = 1 mg/ml, D = 0.5 mg/ml, E = 0.25 mg/ml, F = 0.1 mg/ml, and G = 0 mg/ml.

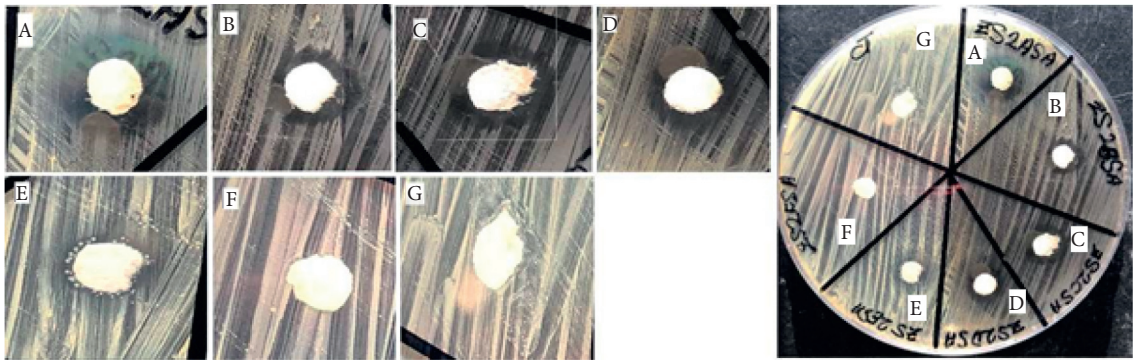

Figure 15: Antibacterial activity of ZnO/Ag nanocomposite against *S. aureus*. The paper disks were impregnated with the following suspension of copper oxide nanoparticles: A = 5 mg/ml, B = 2 mg/ml, C = 1 mg/ml, D = 0.5 mg/ml. E = 0.25 mg/ml, F = 0.1 mg/ml, and G = 0 mg/ml.

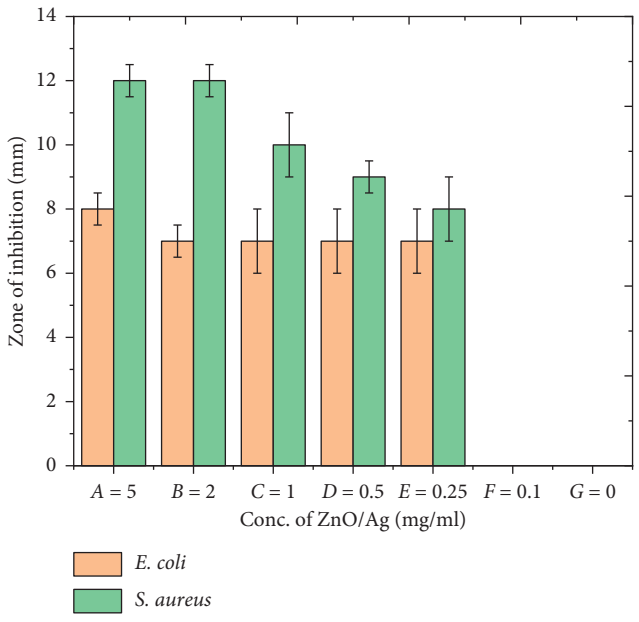

Figure 16: A histogram showing the activity of ZnO/Ag nanocomposite against *E. coli* and *S. aureus*. A = 5 mg/ml, B = 2 mg/ml, C = 1 mg/ml, D = 0.5 mg/ml, E = 0.25 mg/ml, F = 0.1 mg/ml, and G = 0 mg/ml.

The inhibitory activity of CuO/Ag and ZnO/Ag on *E. coli* is demonstrated in Figure 18. The *E. coli* kinetic growth curve shows that the control (without antibacterial agent) sample had relatively high bacteria, which is shown by the exponential rise in its optical density measured at 600 nm. The samples with antibacterial agent show comparably low optical densities compared to their respective control samples as indication of their inhibited growth. The growth kinetic study curves of CuO/Ag nanocomposite recorded lower optical densities than those of ZnO/Ag. CuO/Ag nanocomposite had higher antibacterial activity than ZnO/Ag nanocomposite, which confirms the observation made in the disk diffusion test. The curves of *E. coli* showed higher optical densities than those of *S. aureus*, which are representatives of the sensitivity of *S. aureus* to the antibacterial agents in comparison to *E. coli*. Analytically, both *E. coli* and *S. aureus* strains were more susceptible to CuO/Ag than to ZnO/Ag nanocomposite. Similar observations of the antibacterial performances of CuO/Ag and ZnO/Ag were made in the Kirby–Bauer disk diffusion method in the previous sections of this study.

Figure 19 presents the percentage of bacteria cells that are alive in the inoculum with respect to time. From the kinetic growth study curves, the antibacterial activities of

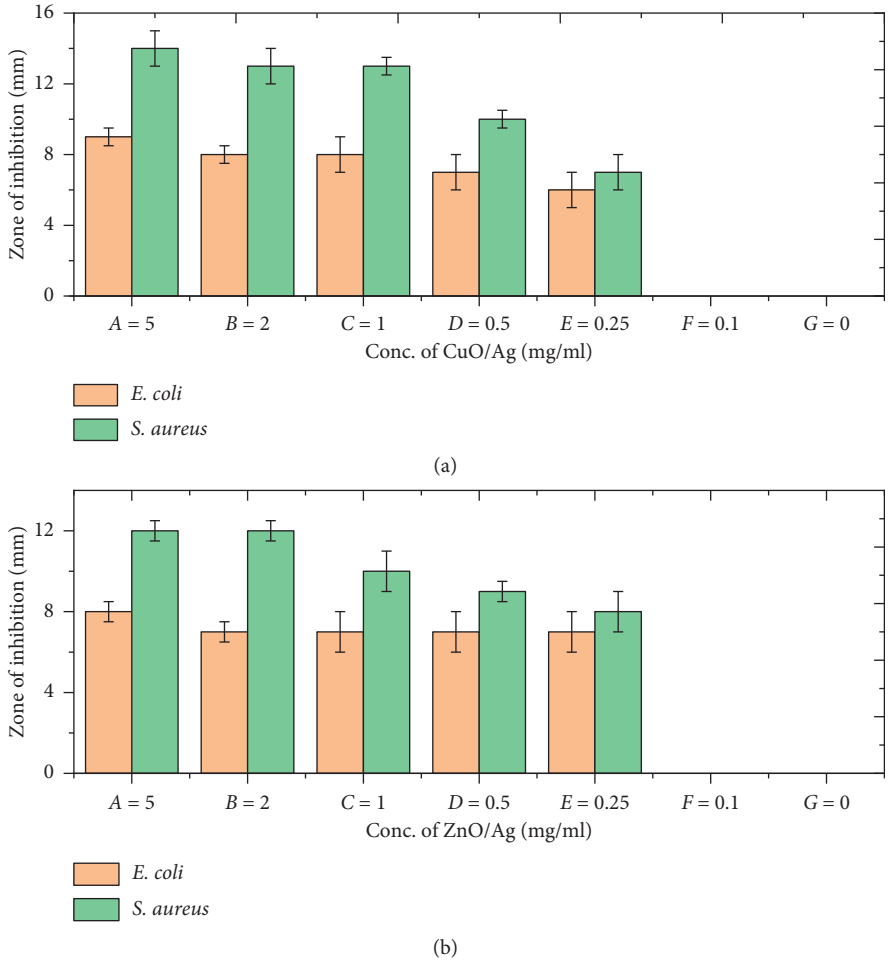

Figure 17: A histogram comparing the activities of (a) CuO/Ag and (b) ZnO/Ag nanocomposites against *E. coli* and *S. aureus*. A = 5 mg/ml, B = 2 mg/ml, C = 1 mg/ml, D = 0.5 mg/ml, E = 0.25 mg/ml, F = 0.1 mg/ml, and G = 0 mg/ml.

Table 2: Minimum inhibition concentration (MIC) values of nanocomposites against bacteria species.

Nanocomposite sample	Minimum inhibition concentration (MIC) (mg/ml)	Minimum inhibition concentration (MIC) (mg/ml)
	E. coli	*S. aureus*
CuO/Ag	0.25	0.25
ZnO/Ag	0.25	0.25

both CuO/Ag and ZnO/Ag nanocomposites on *E. coli* were gradual with respect to time. In the case of both nanocomposites, appreciable effect on *E. coli* was realised from the 18th hour of antibacterial activity. The CuO/Ag antibacterial efficiency on *E. coli* remains almost constant from the 18th hour to the 24th hour. Thus, *E. coli* could not gain resistance or increase in growth in the presence of CuO/Ag after the 18th hour. The antibacterial activity of ZnO/Ag on *E. coli* upon reaching its most downward or steepest peak in the 18th hour saw a slight rise up to the 24th hour. This behaviour of the curves means that the *E. coli* population increased after reaching its minimum in the 18th hour. *E. coli* began to gain resistance against ZnO/Ag after the 18th hour. However, this observation was made about lower concentrations of ZnO/Ag.

The kinetics growth study shows that CuO/Ag and ZnO/Ag had a quicker effect on *S. aureus*. Approximately four hours of antibacterial activity showed a high optimum effect on *S. aureus*. From the growth kinetic curves, it is observed that the CuO/Ag curve saturates approximately from the 4th hour onwards. It can be deduced form this observation that *S. aureus* bacteria cells from this period onward showed no signs of growth in the presence of CuO/Ag antibacterial agents. Thus, the bacteria cells were completely inhibited without any growth potential. On the other hand, *S. aureus* also showed drastic sensitivity by a decrease in cell population after the 4th hour of antibacterial activity against by ZnO/Ag. However, in the presence of lower concentrations (0.25 mg/ml, 0.1 mg/ml, and 0.05 mg/ml) of ZnO/Ag, there was an intermittent slight increase in cell population after

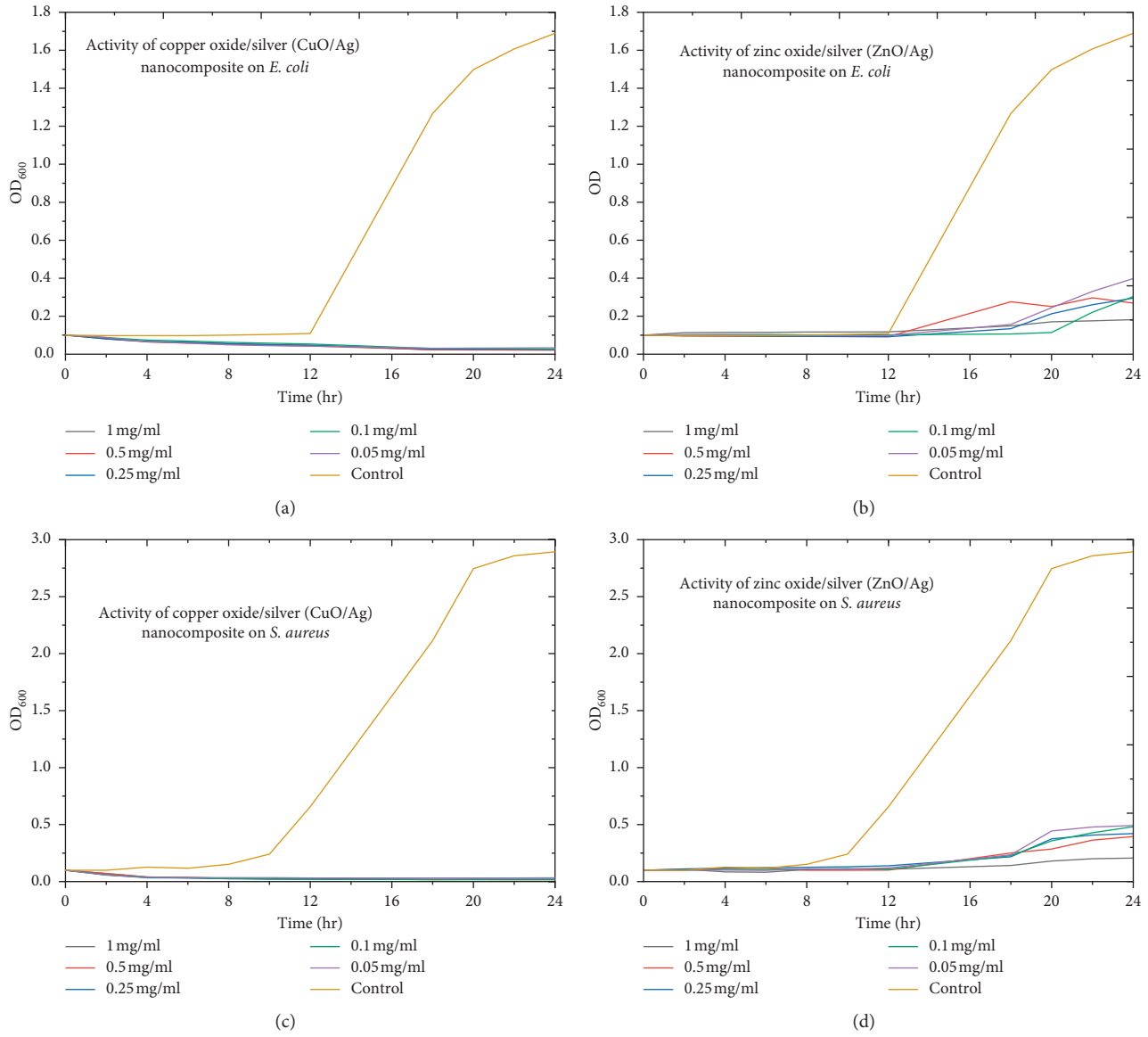

Figure 18: Kinetic growth study on the antibacterial activity of (a) CuO/Ag against *E. coli*, (b) ZnO/Ag against *E. coli*, (c) CuO/Ag against *S. aureus*, and (d) ZnO/Ag against *S. aureus*.

the 4th hour indicated by the gradual rise in the curves. This infers that the *S. aureus* bacteria cells became resistive towards ZnO/Ag antibacterial agents. This rise of the curve again assumed a downward slope, denoting that the cell population began to decrease again. The explanation to this is that, in aqueous medium, zinc oxide dissolves faster than silver, which is partially soluble [38]. Meanwhile, zinc oxide is a micronutrient for cellular metabolism and can be controlled, especially at lower concentrations [39]. However, as the quantity of the partially oxidative silver increases, the cells are again inhibited and assume a downward trend showing a decrease in cell population again.

According to Figure 20, *S. aureus* showed more susceptibility against both antibacterial agents as compared to *E. coli*. After 4 hours of antibacterial activity, *S. aureus* showed significant activity against both antibacterial agents. Meanwhile, *E. coli* recorded major activity against antibacterial agents after 18 hours of antibacterial activity. After 24 hours of antibacterial activity, the efficiencies of the respective nanocomposites were similar for the respective bacteria species. The respective antibacterial efficiency of the microdilution after 24 hours of activity is shown in Table 3. After the 24-hour antibacterial activity, both CuO/Ag and ZnO/Ag had significant activity on both *E. coli* and *S. Aureus*. However, the activity of CuO/Ag was observed to be higher than that of ZnO/Ag among the strains of both species.

Figure 21 is a boxplot demonstrating the antibacterial activities of CuO/Ag and ZnO/Ag against the respective *E. coli* and *S. Aureus* strains after 24 hours of microdilution test. The strains of both species were sensitive to both CuO/Ag and ZnO/Ag. However, CuO/Ag recorded higher activity

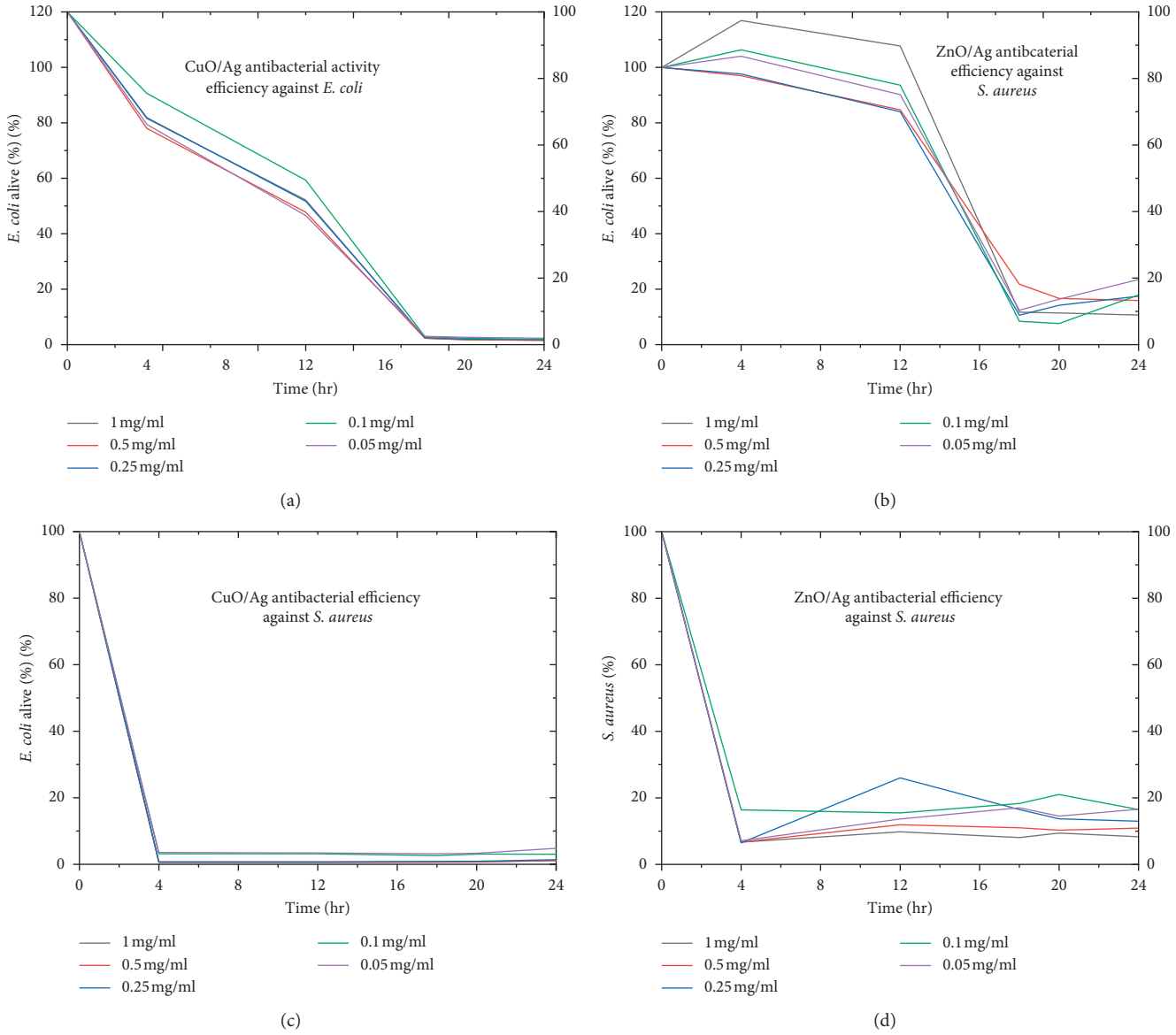

Figure 19: Kinetic growth study on *E. coli* and *S. aureus* that are alive after antibacterial activity by (a) CuO/Ag against *E. coli*, (b) ZnO/Ag against *E. coli*, (c) CuO/Ag against *S. aureus*, and (d) ZnO/Ag against *S. aureus*.

than ZnO/Ag among both species with the difference between their respective mean values being statistically significant at a standard p value of 0.05 using an ANOVA statistical analysis. The results further revealed that the means of CuO/Ag against *E. coli* and CuO/Ag against *S. aureus* had no statistical significance at a p value of 0.05, which suggests that CuO/Ag had a similar activity against both *E. coli* and *S. aureus*, which agrees with their MIC values having the same value of 0.25. The equal MIC values for the strains of both species predict that the nanocomposite antibacterial agent has a similar activity on both bacteria, which was observed in this case. The same observation was made about ZnO/Ag against *E. coli* and *S. aureus*, thus proving the results of the Kirby–Bauer disc diffusion test that the equal MIC values prove that ZnO/Ag had similar activity against both strains of bacteria species. Thus, the nanocomposite antibacterial agents exhibited no strain specificity as they are effective against both the Gram-negative and Gram-positive strains. Strain specificity has been reported by other authors; while *B. subtilis* was susceptible to copper oxide, it was insensitive to silver and also *E. coli* was more susceptible to silver than copper oxide [28].

The enhanced antibacterial activities of the nanocomposites (CuO/Ag and ZnO/Ag) against all the tested bacteria strains show that the synergy created by the nanocomposites produced a wider spectrum of antibacterial activity by being effective against both Gram-negative and Gram-positive bacteria species. The respective nanocomposites had similar effects on both *E. coli* and *S. aureus*.Thus, both CuO/Ag and ZnO/Ag had similar activity on *E. coli* and *S. aureus*. The activity of the different transition metals in the nanocomposites creates a wide spectrum of

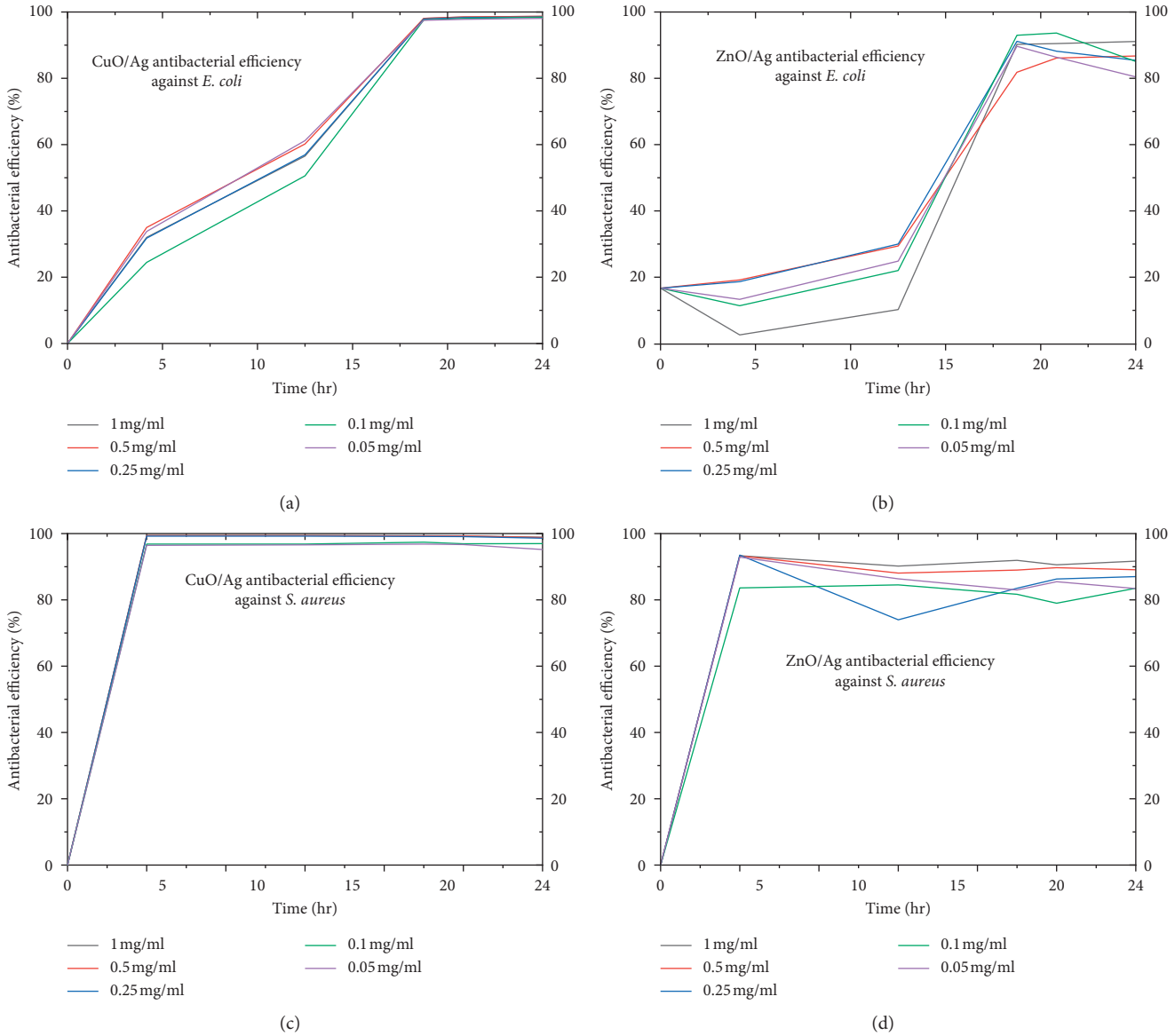

Figure 20: Kinetic growth study on *E. coli* and *S. aureus* that are alive after antibacterial activity by (a) CuO/Ag against *E. coli*, (b) ZnO/Ag against *E. coli*, (c) CuO/Ag against *S. aureus*, and (d) ZnO/Ag against *S. aureus*.

Table 3: The results of microdilution test presenting the relative percentages (%) of bacteria cell death by respective nanoparticles after 24 hours of antibacterial kinetic study. "EC" represents *Escherichia coli*, while "SA" represents *Staphylococcus aureus*.

Conc. of NPs (mg/ml)	Bacteria cell death caused by respective nanoparticles (%)			
	CuO/Ag-EC	CuO/Ag-SA	ZnO/Ag-EC	ZnO/Ag-SA
1	98.7	98.9	89.3	91.7
0.5	98.7	98.8	84.1	89.1
0.25	98.5	98.6	82.5	87
0.1	98.4	96.96	82.1	83.5
0.05	98.1	95.17	76.5	83.4

antibacterial activity by their varying effects against different strains of bacteria species. Nanocomposites combine the toxic effects of the different elemental compositions to create a synergy of antibacterial activity. Bacteria cells have sensitivity to different transition metals. The nanocomposite brought together different transition metals, thereby broadening its spectrum of bacteria susceptibility (antibacterial spectrum).

The respective nanocomposites were fabricated from metal oxide and 1% addition of $AgNO_3$. Ag nanoparticles are

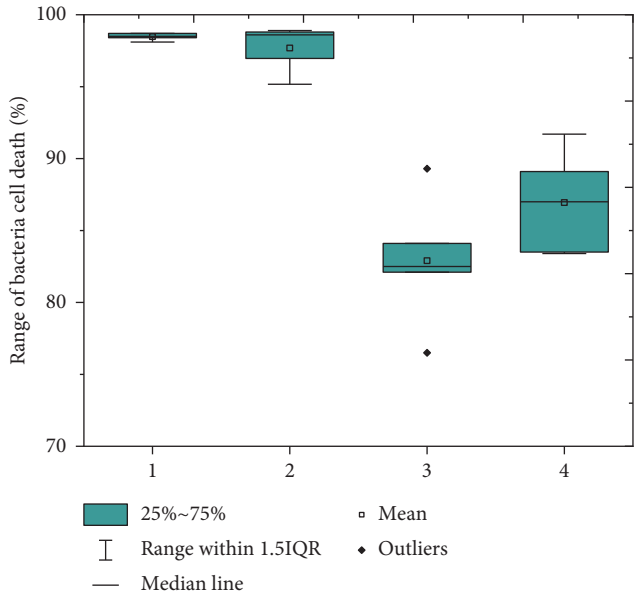

Figure 21: A boxplot of the antibacterial activities of nanocomposites (CuO/Ag and ZnO/Ag) against bacteria species. 1 = CuO/Ag against *E.* coli, 2 = CuO/Ag against *S.* aureus, 3 = ZnO/Ag against *E. coli*, and 4 = ZnO/Ag against *S. aureus*.

relatively expensive than metal oxide nanoparticles. Thus, the creation of the nanocomposite provided a cost-effective highly efficient antibacterial agents.

4. Conclusion

In this investigation, the comparative assessment of the antibacterial activity of silver nanocomposites was carried out through a stepwise procedural approach of synthesis, characterization, and application. The antibacterial activities of CuO/Ag and ZnO/Ag were relatively compared by their activity on Gram-positive and Gram-negative bacteria, which were, respectively, *S. aureus* and *E. coli*. The silver nanocomposites of CuO/Ag and ZnO/Ag were prepared by the simple one pot mixed wet chemical synthesis method. The synthesised nanocomposites were characterised by XRD, XRF, TEM, UV-Vis spectrophotometer, BET, and FTIR. XRD results supported by evidence of the XRF revealed that the synthesised particles were of high purity and the calculation of crystallite size from the highest intensity XRD peak suggested that the particles had identical sizes. The spectrophotometric analysis shows that the prepared CuO/Ag and ZnO/Ag had an enhanced energy band gap different from known CuO and ZnO nanoparticle counterparts, respectively, due to silver doping influences. The TEM analysis of the nanocomposites showed that silver nanoparticles were interspersed within the respective metal oxide nanoparticles. According to the TEM, each nanocomposite had at least single size dimension within 1–100 nm, which defines their nanosize. The BET results further confirmed that the nanocomposites had equivalent surface area and hence particle size as predicted by the XRD spectra analysis of particle size. According to the FTIR spectra, both nanocomposites were devoid of organic surfactants, which could impede antibacterial activities.

The nanocomposites were tested by two main methods of applications. The Kirby–Bauer disc diffusion and the microdilution optical density tests were used to access the antibacterial performance of each nanocomposite by testing them on Gram-positive and Gram-negative bacteria strains including *S. aureus* and *E. coli*. The results showed that CuO/Ag was more effective against both *E. coli* and *S. aureus* as compared to ZnO/Ag. The results further revealed that *S. aureus* was more susceptible to the individual actions of CuO/Ag and ZnO/Ag nanocomposites as compared to *E. coli.*

The results prove the novelty that CuO/Ag nanocomposite has better antibacterial activity against both Gram-positive and Gram-negative bacteria species compared to ZnO/Ag. However, this study can be further extended to study a broader range of bacteria species to further confirm the relative high antibacterial activity of CuO/Ag in comparison to ZnO/Ag.

Data Availability

All data used in this manuscript have been presented within the article.

Conflicts of Interest

The authors declare that they have no conflicts of interest.

References

[1] T. Mukherji and B. G. Eimani, "Investigation of synergistic effect of cuo nanoparticles and nisin on genome of *Escherichia coli* bacteria," *Journal of Water and Environmental Nanotechnology*, vol. 3, no. 4, pp. 355–367, 2018.

[2] A. Ivask, K. Kasemets, M. Mortimer, and A. Kahru, "Toxicity of Ag, CuO and ZnO nanoparticles to selected environmentally relevant test organisms and mammalian cells in vitro: a critical review," *Archives of Toxicology*, vol. 87, no. 7, pp. 1181–1200, 2013.

[3] M. K. Joshi, H. R. Pant, H. J. Kim, J. H. Kim, and C. S. Kim, "One-pot synthesis of ag-iron oxide/reduced graphene oxide nanocomposite via hydrothermal treatment," *Colloids and Surfaces A: Physicochemical and Engineering Aspects*, vol. 446, pp. 102–108, 2014.

[4] S. Park, H. H. Park, S. Y. Kim, S. J. Kim, K. Woo, and G. Ko, "Antiviral properties of silver nanoparticles on a magnetic hybrid colloid," *Applied and Environmental Microbiology*, vol. 80, no. 8, pp. 2343–2350, 2014.

[5] H. Palza, "Antimicrobial polymers with metal nanoparticles," *International Journal of Molecular Sciences*, vol. 16, no. 1, pp. 2099–2116, 2015.

[6] M. Wuithschick, B. Paul, R. Bienert et al., "Size-controlled synthesis of colloidal silver nanoparticles based on mechanistic understanding," *Chemistry of Materials*, vol. 25, no. 23, pp. 4679–4689, 2013.

[7] H. S. Toh, C. Batchelor-Mcauley, K. Tschulik, and R. G. Compton, "Chemical interactions between silver nanoparticles and thiols: a comparison of mercaptohexanol against cysteine," *Science China Chemistry*, vol. 57, no. 9, pp. 1199–1210, 2014.

[8] K. Kalantari, E. Mostafavi, A. M. Afifi et al., "Wound dressings functionalized with silver nanoparticles: promises and pitfalls," *Nanoscale*, vol. 12, no. 4, pp. 2268–2291, 2020.

[9] Thomas Reuters, *World Silver Survey 2015*, Thomas Reuters, Toronto, Canada, 2015.

[10] S. Jagadamma, M. A. Mayes, J. M. Steinweg, and S. M. Schaeffer, "Substrate quality alters the microbial mineralization of added substrate and soil organic carbon," *Biogeosciences*, vol. 11, no. 17, pp. 4665–4678, 2014.

[11] L. Zhang, X. Fu, S. Meng, X. Jiang, J. Wang, and S. Chen, "Ultra-low content of Pt modified CdS nanorods: one-pot synthesis and high photocatalytic activity for H2 production under visible light," *Journal of Materials Chemistry A*, vol. 3, no. 47, pp. 23732–23742, 2015.

[12] C. Zhang, L. Jiang, C. Meng, X. P. Li, and Y. Li, "Ultrasonic-assistant dispersive liquid-liquid microextraction based on solidification of floating organic droplet method for quick determination of polycyclic aromatic hydrocarbons in soils," *Applied Mechanics and Materials*, vol. 190-191, pp. 603–608, 2012.

[13] E. Marzbanrad, *Joining of Silver Nanoparticles : Computer Simulations and Experimental Observations*, University of Waterloo, Waterloo, Canada, 2016.

[14] A. Azam, M. M. Oves, Khan, S. Habib, and A. Memic, "Antimicrobial activity of metal oxide nanoparticles against gram-positive and gram-negative bacteria: a comparative study," *International Journal of Nanomedicine*, vol. 7, pp. 6003–6009, 2012.

[15] G. Carotenuto, M. Palomba, and L. Nicolais, "Nanocomposite preparation by thermal decomposition of [Ag(hfac)(COD)] in amorphous polystyrene," *Advances in Polymer Technology*, vol. 31, no. 3, pp. 242–245, 2012.

[16] S. Huang, D. Ma, Z. Hu et al., "Synergistically enhanced electrochemical performance of Ni3S4–PtX (X=Fe, Ni) heteronanorods as heterogeneous catalysts in dye-sensitized solar cells," *ACS Applied Materials & Interfaces*, vol. 9, no. 33, pp. 27607–27617, 2017.

[17] M. Kokate, K. Garadkar, and A. Gole, "Zinc-oxide-silica-silver nanocomposite: unique one-pot synthesis and enhanced catalytic and anti-bacterial performance," *Journal of Colloid And Interface Science*, vol. 483, pp. 249–260, 2016.

[18] P. Pandey, M. S. Packiyaraj, H. Nigam, G. S. Agarwal, B. Singh, and M. K. Patra, "Antimicrobial properties of CuO nanorods and multi-armed nanoparticles against B. anthracis vegetative cells and endospores," *Archives of Toxicology*, vol. 5, pp. 789–800, 2014.

[19] M. Suleiman, M. Mousa, and A. I. A. Hussein, "Wastewater disinfection by synthesized copper oxide nanoparticles stabilized with surfactant," *Journal of Materials and Environmental Science*, vol. 6, no. 7, pp. 1924–1937, 2015.

[20] E.-S. Jang, "Recent progress in synthesis of plate-like ZnO and its applications: a review," *Journal of the Korean Ceramic Society*, vol. 54, no. 3, pp. 167–183, 2017.

[21] B. Ashe, "*A Detail investigation to observe the effect of zinc oxide and Silver nanoparticles in biological system*," M.S. thesis, National Institute of Technology, Rourkela, India, 2011.

[22] K. S. Khashan, M. S. Jabir, and F. A. Abdulameer, "Preparation and characterization of copper oxide nanoparticles decorated carbon nanoparticles using laser ablation in liquid," *Journal of Physics: Conference Series*, vol. 1003, no. 1, 2018.

[23] A. Taufik and R. Saleh, "Synthesis of iron(II,III) oxide/zinc oxide/copper(II) oxide (Fe3O4/ZnO/CuO) nanocomposites and their photosonocatalytic property for organic dye removal," *Journal of Colloid And Interface Science*, vol. 491, pp. 27–36, 2017.

[24] S. P. Rajendran and K. Sengodan, "Synthesis and characterization of zinc oxide and iron oxide nanoparticles using sesbania grandiflora leaf extract as reducing agent," *Journal of Nanoscience*, vol. 2017, Article ID 8348507, 7 pages, 2017.

[25] S. Kumar, D. V. N. S. Pamidimarri, D. Young, and J. Na, "Y-doped zinc oxide (YZO) nano fl owers , microstructural analysis and test their antibacterial activity," *Materials Science & Engineering C*, vol. 53, pp. 104–110, 2015.

[26] D. E. Anderson, S. Balapangu, H. N. A. Fleischer et al., "Investigating the influence of temperature on the kaolinite-base synthesis of Zeolite and Urease immobilization for the potential fabrication of electrochemical urea biosensors," *Sensors (Switzerland)*, vol. 17, no. 8, 2017.

[27] A. Stewart, S. Zheng, M. R. McCourt, and S. E. J. Bell, "Controlling assembly of mixed thiol monolayers on silver nanoparticles to tune their surface properties," *ACS Nano*, vol. 6, no. 5, pp. 3718–3726, 2012.

[28] K.-Y. Yoon, J. Hoon Byeon, J.-H. Park, and J. Hwang, "Susceptibility constants of *Escherichia coli* and Bacillus subtilis to silver and copper nanoparticles," *Science of The Total Environment*, vol. 373, no. 2-3, pp. 572–575, 2007.

[29] J. P. Ruparelia, A. K. Chatterjee, and S. P. Duttagupta, "Strain specificity in antimicrobial activity of silver and copper nanoparticles," *Acta Biomaterialia*, vol. 4, no. 3, pp. 707–716, 2008.

[30] L. R. Muslimin, F. Nainu, and R. Himawan, "Antibiotic sensitivity pattern of *Staphylococcus aureus* and *Escherichia coli* isolated from bovine fresh milk," *Jurnal Veteriner*, vol. 16, no. 4, pp. 520–524, 2015.

[31] M. F. Elkady, H. Shokry Hassan, E. E. Hafez, and A. Fouad, "Construction of zinc oxide into different morphological structures to be utilized as antimicrobial agent against multidrug resistant bacteria. bioinorganic chemistry and applications," *Bioinorganic Chemistry and Applications*, vol. 2015, Article ID 536854, 20 pages, 2015.

[32] D. S. Handayani, Pranoto, D. A. Saputra, and S. D. Marliyana, "Antibacterial activity of polyeugenol against staphylococcus aureus and escherichia coli," *IOP Conference Series: Materials Science and Engineering*, vol. 578, no. 1, 2019.

[33] S. Bashir, K. Chamakura, R. Perez-Ballestero, Z. Luo, and J. Liu, "Mechanism of silver nanoparticles as a disinfectant," *International Journal of Green Nanotechnology*, vol. 3, no. 2, pp. 118–133, 2011.

[34] M. Roberson, V. Rangari, S. Jeelani, T. Samuel, and C. Yates, "Synthesis and characterization silver, zinc oxide and hybrid silver/zinc oxide nanoparticles for antimicrobial applications," *Nano LIFE*, vol. 4, no. 1, p. 1440003, 2014.

[35] A. Yoo, "Effect of zinc oxide and silver nanoparticles on intestinal bacteria," M.S. thesis, University of Missouri, Columbia, MO, USA, 2013.

[36] R. K. Oshiro, *Method 1604: total coliforms and Escherichia coli in Water by Membrane Filtration using a Simultaneous Detection Technique (MI Medium)*, p. 18, U.S. Environmental Protection Agency, Washington, DC, USA, 2002.

[37] S. K. Verma, E. Jha, P. K. Panda et al., "Mechanistic insight into size-dependent enhanced cytotoxicity of industrial antibacterial titanium oxide nanoparticles on colon cells because of reactive oxygen species quenching and neutral lipid alteration," *ACS Omega*, vol. 3, no. 1, pp. 1244–1262, 2018.

[38] C. L. Ho, R. Chen, H. Sun et al., "Silver nanoparticles: partial oxidation and antibacterial activities," *JBIC Journal of Biological Inorganic Chemistry*, vol. 12, no. 4, pp. 527–534, 2007.

[39] C. M. Dozois, "Iron, copper, zinc, and manganese transport and regulation in pathogenic Enterobacteria : correlations between strains, site of infection and the relative importance of the different metal transport systems for virulence," *Frontiers in Cellular and Infection Microbiology*, vol. 3, pp. 1–24, 2013.